EMAS Engineering Modelling, Analysis & Simulation
THE NAFEMS JOURNAL

NAFEMS

Vol. 1, Issue 1, 2024

A novel numerical analysis method for predicting non-Newtonian lubricant (grease) distribution in ball bearings

M. Pandya[a,1], P. Tesini[b], F. Bogliacino[c], F. Mandrile[c]

[a]SKF, Plot 2, Bommasandra Industrial Area, Hosur Road, Bangalore 560099, India
[b]SKF, Meidoornkade 14, Houten 3992 AK, Netherlands
[c]SKF, Via Pinerolo, 44, Airasca (TO) 10060, Italy

Abstract

Grease is a visco-elastic fluid and the most common lubricant for rolling bearings. During the churning phase (initial phase) of bearing operation, most of the grease is collected at various locations in the bearing, e.g. by the seal, at the bottom cage bar, in the cage pockets, which are then called grease reservoirs. These are formed based on bearing operating conditions, grease type, bearing geometry, bearing type. The grease reservoirs supply lubricant to the bearing contacts via bleeding: during operation the oil bleeds out of the reservoirs and lubricates the contacts. Since the distribution of grease is crucial to the bearing lubrication, the design of bearing components e.g., the cage, shall aim at an optimal grease reservoir creation during the churning phase. It is difficult to observe the effect of component design on the grease distribution through real life experiments, so CFD simulations with MPS (Moving Particle Semi-implicit) method are performed here. Flow Simulations with MPS method can help determine the factors influencing the grease distribution inside the bearing after churning, with the final aim of enhancing lubrication. For the current simulations, a CAE software based on MPS, namely Particleworks, was used.

Grease consists of a base oil, a thickener, and additives. Since it is a non-Newtonian fluid, it has a nonlinear relation shear stress vs shear rate. It is a visco-elastic material, so it does not flow in the absence of a threshold force. For current simulations, the grease rheology has been modelled using the Herschel-Bulkley model. The model was fitted on in-house rheometer test data and was reduced to a single cage-ball segment. All critical kinematic properties were preserved, that is the speeds of both the inner ring and ball surfaces and the oscillation of the ball position within the pocket as it travels through the loaded and unloaded zones of the bearing. The location and the duration of grease injections resulted in different grease distributions in the model. For demonstration purposes, this document only focuses on the results obtained injecting a grease layer on the inner ring surface in front of the contact. This realistically predicted grease reservoirs to be located at the cage bottom, on the top of cage and in the cage pockets. Sensitivity study on particle size, time step, surface tension and the parametric variation of the bearing speed were also performed. This is an important milestone, as we are able for the first time to virtually simulate the onset of grease reservoirs at locations corresponding to evidence from real bearing operations. The distribution of grease observed at the cage pockets is very important for oil film replenishment. This outcome gives us confidence that the MPS method can be used to support the design of bearing components contributing to enhanced lubrication.

Keywords

lubrication, friction, wear, non-Newtonian behaviour, grease, bearing, ball bearing, oil, MPS, CFD, failure

[1]Corresponding author.
E-mail address: mehul.p.pandya@skf.com
https://doi.org/10.59972/nru3jt68

1 Introduction

Inefficient lubrication is regarded as a major cause of bearing failure, so it becomes important to understand whether a bearing is properly lubricated or not. The lubricant in bearings serves different purposes: to reduce friction and wear, to carry away the heat generated due to friction, to protect the surfaces from corrosion. The first step in the lubrication selection process for any bearing application, is to select grease or oil. Although both can fulfil the purpose, each of them provides special advantages and comes with certain limitations. Grease lubrication has certainly clear advantages over oil lubrication as described by Lugt [1]. Grease does not leak easily; it has sealing properties and protects the bearing surfaces from fretting and corrosion due to its tendency to adhere to surfaces. On the other hand, circulating oil can be used to remove heat from the bearing in high temperature applications.

Grease lubrication is a process in which several phases are identified: initial churning, bleeding and severe film break down. During the churning phase, the grease is pushed into the 'unswept volume' of the bearing (onto the seals or onto bearing shoulders) and ends up sticking to the cage as shown by Lugt [1]. Part of the grease pushed into the unswept volume will no longer actively participate to the lubrication process, leaving only a limited grease active quantity available, positioned at various locations, also based on the bearing type. This grease active volume strongly influences the remaining lubrication in the bearing. The distribution of this volume is determined by the grease flow, which is very complex to model due to the strong non-linear rheology, and that's where such simulations are especially useful. The grease bleeding will supply oil to the raceway contacts: either it bleeds oil due to severe shear on the raceway or small fresh quantities of grease may be sheared off from the volume stored on the shoulder. Tomonobu Komoriya et al. [3] carried out an experimental investigation on angular contact ball bearing lubricated with urea greases and observed lumps of grease created on the front face of the outer ring, on the shoulder of outer ring, on the inner surface of the cage, on the shoulder of the inner ring. These lumps served as grease reservoir and oil bled from here migrated to lubricate the raceways. Takashi Noda et al. [2] used an X-ray computed tomography (CT) imaging system to capture the grease distribution and the grease internal flows in a ball bearing. Additionally, Takashi Noda performed numerical simulations of the grease flow: CFD for the macroscopic flow and elasto-hydrodynamics for microscopic film thickness variation in the contact area. This investigation explored the complicated grease behaviour and the film thickness in a ball bearing. The grease distribution and lubrication transition were visualised and quantified. An integrated multi-scale grease flow simulation scheme was targeted as the final goal of this work.

No study seems to be available on the prediction of the grease flow inside bearings by means of simulation. So, this study is targeting the prediction of the reservoir locations within a ball bearing. It is expected that reservoirs:

- collect large amount of grease and,
- release lubricant towards bearing contacts.

Predicting the formation of reservoirs with the help of simulations can help designing greased bearings with improved lubrication features.

2 Grease distribution in bearing and reservoir formation

The grease distribution in a bearing is dependent on the bearing design. The consistency of grease prevents it from leaking out of the bearing, but it might also prevent optimal lubrication. The grease lubrication of bearings has three typical phases as shown by Lugt [1]. After the initial filling or during relubrication, the grease will fill the space between the rolling elements. During the churning phase, the grease is pushed into the unswept volume of the bearing (onto the seals or onto the ring shoulders) and will partly stick to the cage. For Angular Contact Ball Bearings (ACBB), the grease is mostly collecting on the larger outer ring shoulder of the bearing, the seals, and the cage bar. For Deep Groove Ball Bearings (DGBB), the grease is mainly collecting on the seals, in between outer and inner ring. As observed by Chatra and Lugt [4], who performed tests on DGBB (designation 6204-2Z/C3), about 35 % of the initial grease was left inside the bearings in their experiments. Most of the grease was attached to the seals at the end of the churning phase. During the next phase, which is called bleeding phase, the grease will slowly provide the raceways with lubricant by either shearing or bleeding. During this phase, the lubricating film will be governed by a feed and loss mechanism, where

the raceways are fed by grease from the reservoirs but will also lose the lubricant due to side flow and oxidation. This may lead to starvation. A schematic of this process is shown in Figure 1.

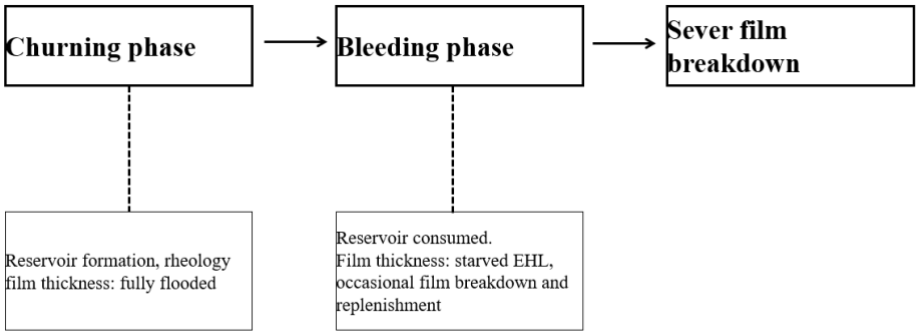

Figure 1. Different phases of grease lubrication in a bearing application.

3 Grease rheology and rheology models

Rheology is the study of how materials flow as function of the shear or the load. Temperature, pressure, shear rate and its duration may also affect the rheological properties of a material. The thickener in the grease has the function of enhancing its tackiness to surfaces and limiting leaking and squeezing under pressure. At the same time, the grease should also be able to flow into the bearing for efficient lubrication. Lubricating grease consists of 65÷95% base oil, 3÷30% thickener and 0÷10% additives. The interaction between the oil and the thickener determines the flow properties, so the rheology of the grease. In addition to this, important aspects of the grease behaviour in bearings are also (1) to form the reservoirs (locations in the bearing, where grease collects for longer time depending on bearing type, geometry, operating conditions) and (2) to release the lubricating oil towards the bearing contacts from these reservoirs. At higher shear rates, a grease behaves similarly to oil, but at lower shear rates it behaves like a viscoelastic solid.

Rheological models used to characterize the fluid flow are classified as Newtonian and non-Newtonian. The Newtonian model describes the simplest fluid flow behaviour, where viscosity is linear constant of proportionality between shear stress and shear rate. Such fluids start to flow immediately, and the shear stress increases as the shear rate increases. Many fluids are non-Newtonian fluids though. The viscosity of a non-Newtonian fluid is not constant at a given temperature and pressure but depends on flow conditions like the shear rate, the flow geometry, the history of deformation. They present a time dependent viscosity and exhibit a different relationship between shear rate and shear stress. So, a constant coefficient of viscosity η cannot be measured. Non-Newtonian fluids be classified into three classes. Time independent fluids or generalized Newtonian fluids for which the shear rate at any point is determined by the value of the shear stress at that point at that instant. Time dependent fluids for which the shear rate vs. shear stress relation depends on the duration of shearing and history. Visco-elastic fluids, which show both ideal and elastic solid behaviour.

Figure 2 shows a schematic representation of various rheological behaviours of fluids and the behaviour of grease viscosity over shear rate and most of the models. A fluid with increasing viscosity when the shear rate is increased is called dilatant (shear thickening fluid). A fluid with decreasing viscosity when the shear rate is increased is called pseudoplastic (shear thinning fluid). Bingham fluids like Casson fluid and plastic show a yield stress and fluid flow that only occur when external stresses are larger than the yield stress. This can be plastic or pseudoplastic (Casson fluid). Greases show Bingham like behaviour (Casson fluid and plastic). It behaves like elastic solid as far as the external stress is below the yield stress. When the yield stress is exceeded, it starts to flow. So, plastic behaviour with constant viscosity or a pseudoplastic behaviour with decreasing viscosity and increasing shear rate can occur.

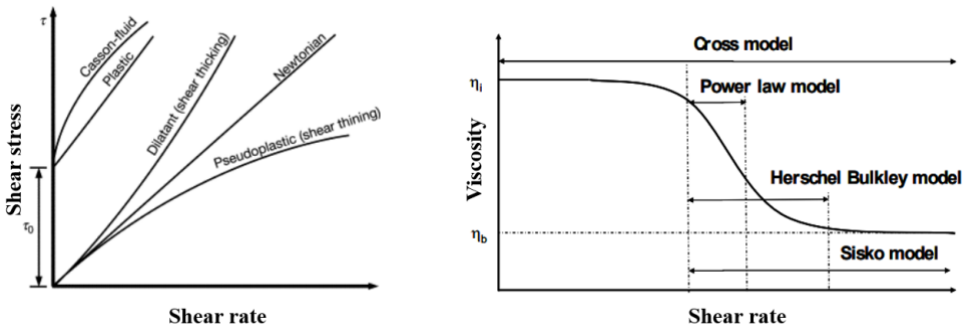

Figure 2. Grease rheology models.

The applicability of a model depends on the range of measured data or the region of the behaviour of interest. There are different models: Cross, Power law, Herschel-Bulkley, Sisko. The Herschel-Bulkley model is preferred to other models because it is the most advanced and results in accurate rheological behaviour when adequate experimental data is available. In this analysis the grease rheology has been modelled using the Herschel-Bulkley model. The Herschel-Bulkley model is formulated as

$$\sigma_{HB} = \tau_{yield} + K\dot{\gamma}^{n} \quad + \eta_0\dot{\gamma} \tag{1}$$

where σ_{HB} is the shear stress, τ_{yield} is the yield stress, K is the consistency coefficient; n is the flow index, $\dot{\gamma}$ is the shear rate (or velocity gradient), η_0 is the base oil viscosity.

A rheometer is used to measure the rheology of fluids like greases. It is an instrument to measure the viscosity for those fluids which cannot be defined by single viscosity and therefore require more parameters to set and to be measured than the viscometer. The rheometer of an SKF laboratory was used to measure the grease rheology of a selected grease. The model was fitted on in-house rheometer test data. The viscosity model in Particleworks was implemented dividing equation (1) by the shear rate. It is to be noted that when the shear rate vanishes the viscosity tends to infinity. That means that viscosity will diverge at zero shear rate. However, the higher the viscosity the smaller the numerical time step required for stability and, therefore, the viscosity model had to be capped. The maximum viscosity was obtained for a minimum shear rate of 1e-06.

Note that this is an important limitation of the numerical viscous model since it is unable to model the shear stress of zero shear rate of the lubricant. That means that the tendency of a grease lump to maintain its shape indefinitely, when it is not subjected to external forces, cannot be modelled.

4 Moving Particle Semi-implicit method

Particleworks is a Moving Particle Semi-implicit (MPS) based CFD software package [5]. MPS method solves Navier-Stokes equations in a Lagrangian framework. Here the fluid is represented by particles and, therefore, it can simulate accurately splashing and free surface flows. It was originally proposed by Prof. Koshizuka at the university of Tokyo [5]. This method handles complex boundary problems easily. This method was born from SPH (Smooth Particle Hydrodynamics). SPH method may not be suitable for incompressible fluids, as it was formulated based on compressible fluid dynamics. While the MP Semi-implicit (or fully implicit) solver is best suited to solve incompressible fluids.

The continuity equation (mass conservation law) is written as

$$\frac{D\rho}{Dt} = 0. \tag{2}$$

The Navier-Stokes equation (momentum conservation law) can be expressed as

$$\frac{D\vec{u}}{Dt} = -\frac{\nabla P}{\rho} + \vartheta\nabla^2\vec{u} + \vec{g}, \tag{3}$$

where $\frac{D\vec{u}}{Dt}$ expresses a Lagrangian derivation, ρ is the density, $\vec{u}$ is the velocity, P is the pressure, ϑ is the kinematic viscosity coefficient and $\vec{g}$ is the gravity direction.

In the MPS method, the Navier-Stokes equations are divided into two stages, and all terms are solved explicitly, except the pressure term, which is solved implicitly.

An explicit calculation of terms except the pressure term can be formulated as

$$\frac{\vec{u}^{*}-\vec{u}^{k}}{\Delta t}=\vartheta\nabla^{2}\vec{u}^{\mathrm{k}}+\vec{g}\,. \tag{4}$$

Pressure can be implicitly calculated as

$$\nabla^{2}P^{k+1}=\frac{\rho}{\Delta t^{2}}\frac{n^{*}-n^{0}}{n^{0}}. \tag{5}$$

Velocity and position correction by the pressure gradient can be expressed as

$$\frac{\vec{u}^{k+1}-\vec{u}^{*}}{\Delta t}=\frac{\nabla P^{k+1}}{\rho}, \tag{6}$$

where n is particle number density, and n^{0} is the particle number density at the initial state. Subscript *k* refers to the timestep. Superscript * refers to the physical quantity at the stage where explicit calculation has been completed.

When the surface tension model is used, fluid particles are in motion while satisfying the following Navier-stokes equation

$$\frac{D\vec{u}}{Dt}=-\frac{\nabla P}{\rho}+\vartheta\nabla^{2}\vec{u}+\vec{g}-\nabla\emptyset. \tag{7}$$

The fourth term on the right-hand side of the above equation is the surface tension term of the potential model. In addition, the gradient model of the particle method is not used for the fourth term, which is calculated by

$$\nabla\emptyset=\sum_{j\neq i}\frac{d\emptyset}{dr}\frac{\vec{r}_{ij}}{|\vec{r}_{ij}|}, \tag{8}$$

$$\emptyset=C\emptyset, \tag{9}$$

where *i, j* are particle numbers, $\overrightarrow{r_{ij}}$is the position vector from particle *i* to particle *j*, $\emptyset$ is the potential energy. *C* is the potential coefficient that determines the level of potential force, and its value is proportional to the coefficient of surface tension of the liquid.

The potential force between two particles is calculated by following equation:

$$\emptyset(|\vec{r}_{ij}|)=\frac{C}{3r_{e}^{2}}(|\vec{r}_{ij}|-r_{e})^{2}\left(|\vec{r}_{ij}|+\frac{1}{2}r_{e}\right), \tag{10}$$

where C is the potential coefficient that determines the level of force. The potential coefficient is calculated with the following equation:

$$C=\frac{138\sigma}{\rho l_{0}^{2}\left(\frac{r_{e}}{l_{0}}\right)^{5}}, \tag{11}$$

where l_0 is the initial particle distance, r_e is the effective radius and its default value is *3.1* l_0.

In addition to this, consideration can be given to wettability by changing the ratio of the potential force given to particles and the potential force given to the interaction between fluid particles and wall. From the contact angle of wettability θ and the Equation 14 the potential coefficient between fluid particles C_f is calculated. From this obtained coefficient, the potential coefficient between fluid and wall C_{fs} is calculated by the following equation.

$$\frac{C_{fs}}{C_{f}}=\frac{1}{2}(1+cos\theta) \tag{12}$$

The potential force between different fluids is calculated with a coefficient obtained by multiplying the harmonic average of individual potential coefficients by parameter (coefficient of potential). The potential coefficient between fluid and wall is also multiplied by a parameter (coefficient of potential).

5 Analysis model setup

This section describes the steps to create a CFD model by identifying the geometry taken into consideration, establishing the input parameters, setting the operating conditions, the particle size study, the simulation strategy to model the cage oscillations, the surface tension and monitoring the grease quantity to interpret the results.

5.1 Segmented model

Simulating the full model of a bearing is always time consuming and challenging. So, a simplified CFD model (only one ball-cage segment) was built, as shown in Figure 3. The developed model reduction makes use of the axial-rotation periodicity of the problem. This approximation also allowed to reduce the particle size, therefore improving the resolution of the model.

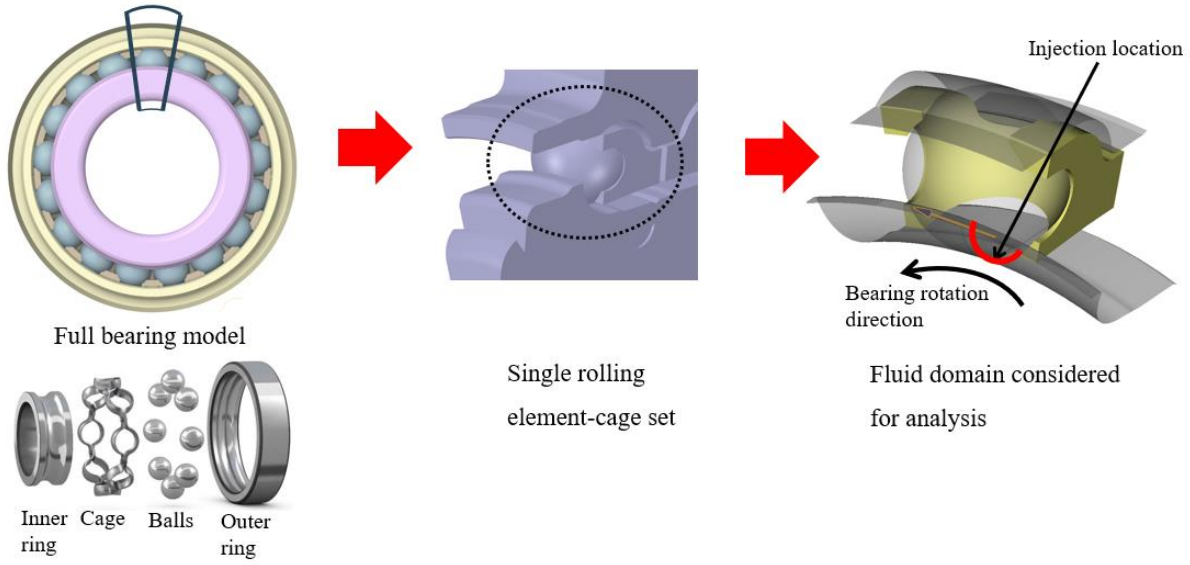

Figure 3. CFD model details

5.2 Injection

A thin layer of grease was injected (placed on IR as shown by red arc in Figure 3 with the assumption of travelling at the same speed of IR. Obviously, alternative injection methods e.g., on the OR, on the top or the bottom of the cage, are possible. These alternatives are outside the scope of this paper.

5.3 Bearing speed

The speeds presented in Table 1 were selected to assess the grease reservoir formation under realistic operating conditions. The ball rotates around its own centre with the specified speed, while the IR rotates around the bearing centre. All these conditions are modelled by taking the cage as reference.

Table 1. Operating conditions, grease flow.

Bearing speed level	IR speed (rpm)	Ball speed (rpm)	Grease temperature (°C)
Lower	300	820	
Medium	600	1638	40
Higher	900	2457	

5.4 Cage oscillations modelling

The cage has the main function of guiding the balls as they travel around the bearing axis. When the ball is in the unloaded zone of the bearing, it is pushed by the cage. When the ball enters the loaded zone, it tends to accelerate and pushes the cage forward. This relative motion (the ball moves within the cage pocket) was modelled (Figure 4) by creating a displacement function, which depends on the clearance between the pocket and the ball, the contact angle, the IR radius, and the IR speed.

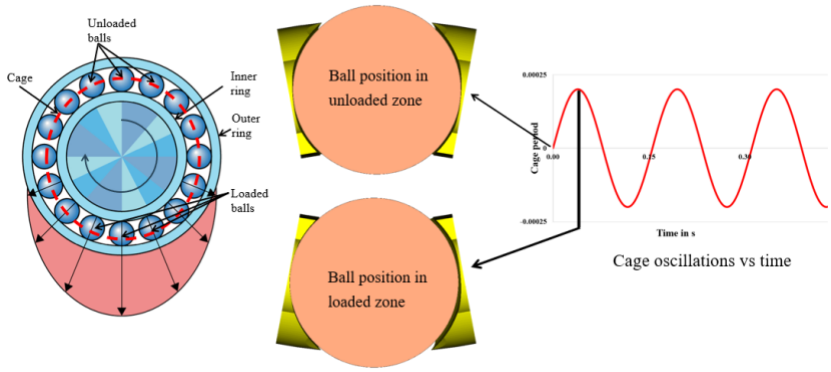

Figure 4. Cage oscillations.

5.5 Particle size

The particle size in Particleworks is determined considering the required spatial resolution, the smallest gap size, the computation time, and the accuracy needed. At the point in time when the analyses were performed for this study, the software did not have adaptive particle size capability, so a compromise was taken to select the most suitable particle size. Adaptive particle size is the capability to model critical areas with smaller (fine) particle size for better resolution and precision while modelling other uncritical areas with larger (coarse) particle size and so saving computational time, which can be utilized to carry out more studies or verify more designs. In absence of this feature, an iterative particle size study was performed where various sizes of particle were taken for each iteration and the number of particles between small gaps like cage and ball were measured for each iteration. The larger the particle size, the more particles are escaping from the fluid domain giving less precision. Smaller particle size gives better precision. The precision was measured in terms of smooth variation of grease velocity from cage to rolling elements. The gap between the cage and the ball is about 0.2 mm. This sensitivity study on the particle size concluded that 0.02 mm is the best compromise as it provides a sufficient resolution for the grease flow with 5 to 6 layers in the cage pocket as shown in Figure 5.

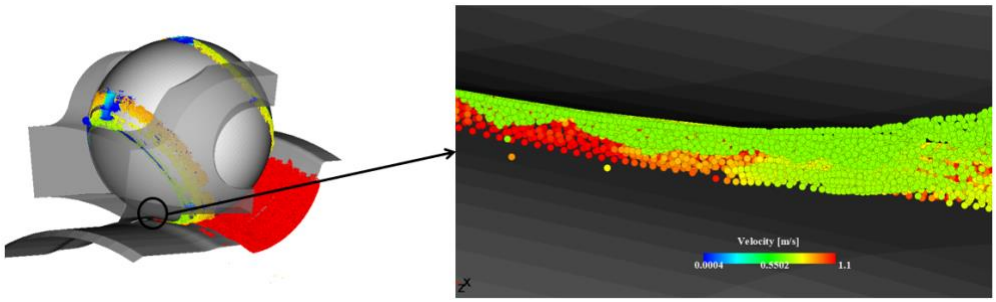

Figure 5. Particle resolution at small gaps.

5.6 Surface tension modelling

The surface tension was modelled using the potential model, i.e. by adding an attraction force between the particles. The surface tension coefficient is an important parameter for the balance between shear and surface tension forces.

Grease sticks to the surface of the ball and the cage if the volume forces are lower than the shear stress at zero shear rate. Since shear stress at zero shear rate cannot be modelled via a finite viscosity, the potential model of surface tension was used instead. An iterative study was performed with different surface tension coefficients varying from 0.005 N/m to 0.072 N/m. It was observed that 0.005 N/m was sufficient to model the required adhesion of the lubricant on the moving surfaces without causing alteration to the shape of grease reservoirs, e.g., producing unphysical drops or clamps.

5.7 Monitoring the grease quantity

The grease was injected for a limited time (until the end of first cage period) and its behaviour was monitored until the stabilisation of the grease quantity in the reservoirs. Figure 6 shows the grease

quantity vs IR revolutions for a specific reservoir. As can be seen, the grease quantity is stable after 15 to 20 revolutions. So, it is prudent to stop the simulation at the end of 45 revolutions.

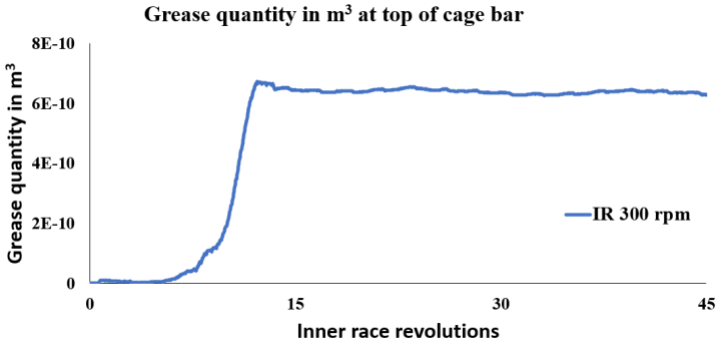

Figure 6. Amount of grease quantity in reservoirs.

6 Results

In this section, the simulated grease flow distribution is investigated at various locations in the bearing model. This simulation model predicts the formation of two main grease reservoirs, at the bottom of the cage bar (64.5 %) and at the top of the cage bar (33.6 %). Other reservoirs (e.g., within the cage pocket) consist of extremely small grease quantities.

The specific grease distribution is also dependent on the position of the ball when the injection occurred and on the position of the injection. Here just one configuration is presented.

Figure 7 shows on left side the percentage of grease at the mentioned reservoir locations and the grease distribution in blue on the right side. The data plotted in this picture is the average grease quantity in the reservoirs for all bearing speeds simulated. The representation on right side is clipped: the grease particles with velocity values higher than 0.001 m/s are not shown. The grease having lower velocity than 0.001 m/s either flows extremely slowly or is stationary at the reservoir.

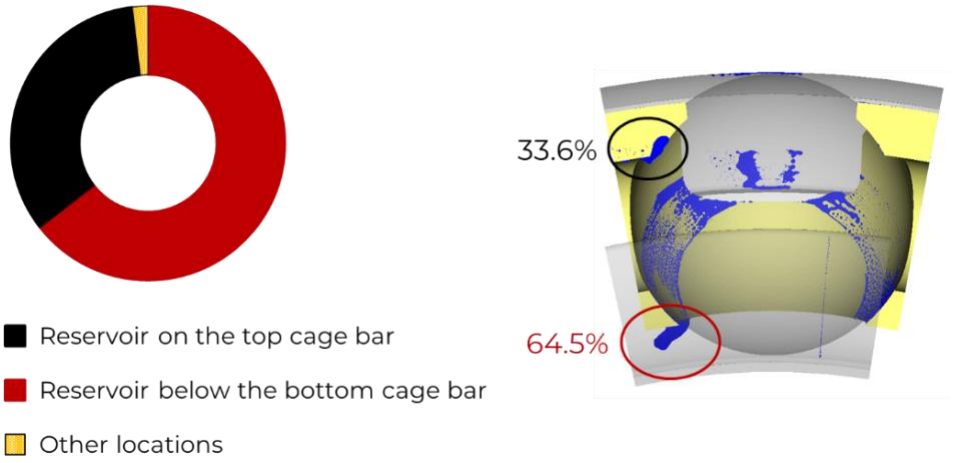

Figure 7. Percentage of grease quantity in reservoirs.

A detailed investigation is required to understand how the grease accumulates at these locations, so it was decided to visualise the initial grease shearing and the subsequent steady state flow. Figure 8 shows (A) the grease flow velocity plot after few revolutions of the IR and (B) the grease flow after completing 30 revolutions of IR. It is observed that some grease is scraped as soon as it meets on the lower cage bar. The blue colour shows extremely small velocity (close to 0 m/s) and it either indicates grease stuck in the cage pocket or accumulated under the cage bar. It is interesting to observe that grease collects under the bottom cage bar and on top of the cage bar for all speeds. The bottom cage bar receives more grease at higher operating speeds than when the speed is low. The upper cage bar receives more grease for lower speed than higher speed. It is also observed that the width of the grease layer sticking to the ball surface reduces as the speed increases. The visualization of the grease flow is required to understand the formation of reservoir for various speeds. The velocity of scraped grease

below the lower cage bar is shown in Figure 9. The higher the speed, the higher the amount of grease sticking on the ball, therefore the larger the reservoir scraped by the lower cage bar. However, the higher the speed, the narrower is the grease band sticking on the ball, therefore at high speed less grease can be scraped by the top cage bar, as shown by Figure 9.b. Figure 9.c shows the steady state condition, when the shearing and scraping has stabilised and the reservoirs have formed. The dependency of the grease behaviour on the IR speed derives from the relation between the viscosity and the shear rate. The higher the speed, the lower the viscosity of the lubricant in the ball-raceway contact. This suggests that the described methodology can be successfully applied to compare different greases as well.

It is also important to observe the grease behaviour in the cage pocket. Figure 10 shows the grease quantity (plot clipped at grease speed 0.001 m/s) becoming stable in the cage pocket for the 300-rpm case. Figure 11 shows the grease flow in the cage pocket for various speeds and at different timesteps. It is observed that most of the grease is scraped on left side of the cage, opposite to the direction of IR rotation.

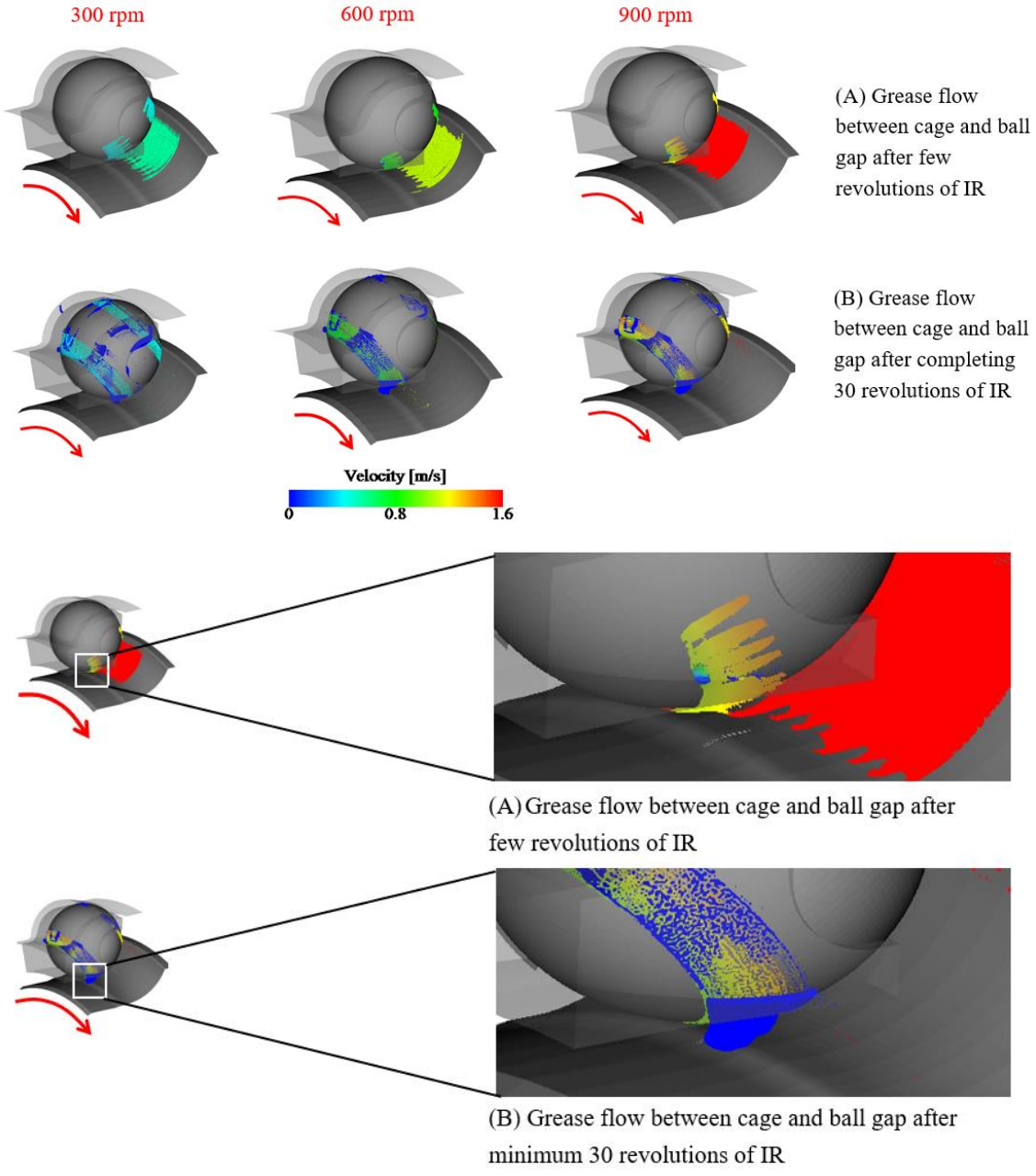

Figure 8. Grease flow around the ball.

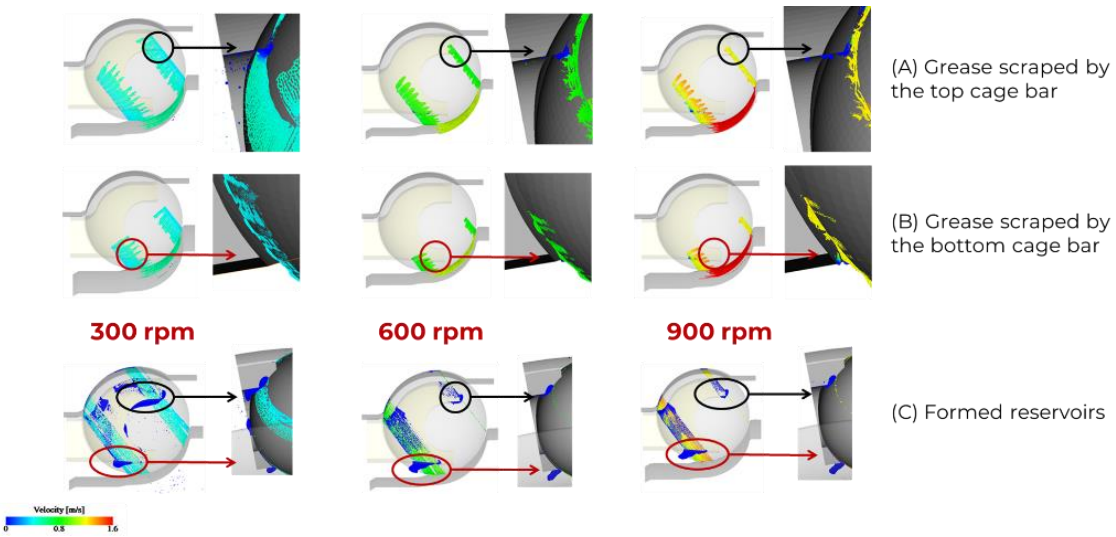

Figure 9. Scraping of grease by the cage bars.

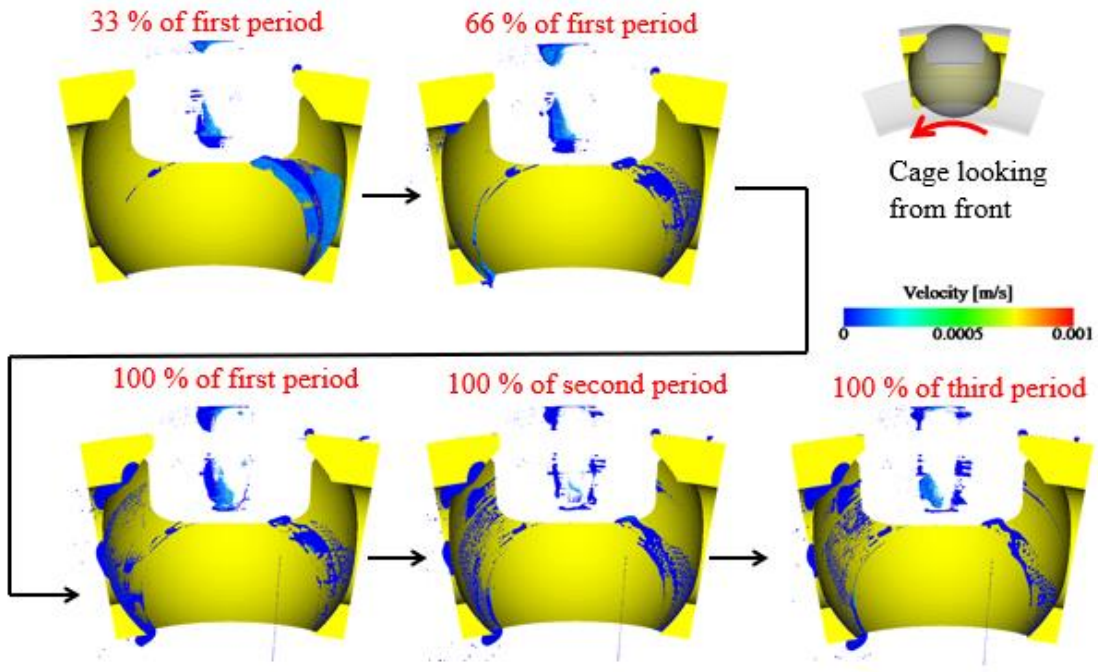

Figure 10. Grease flow in the cage pocket (clipped plot).

Figure 12 shows the grease accumulation (grease quantity in m3) in the different reservoirs over the IR revolutions. The blue grease lumps shown in the red circles are grease reservoirs formed by scraping. It is observed that:

- The bottom of cage bar accumulates most of the grease when the bearing speed is high. With lower speed, the grease quantity in this reservoir reduces.
- The top of cage bar accumulates most of the grease when speed is low. As the speed increases, the grease quantity in this reservoir reduces.

At the current moment no visual inspection of this specific bearing cage has been carried out yet. However, several experimental results demonstrate that grease forms reservoirs below and above the cage bar and on the sides of the raceways. Therefore, these results show that it is possible to predict the formation of grease reservoirs.

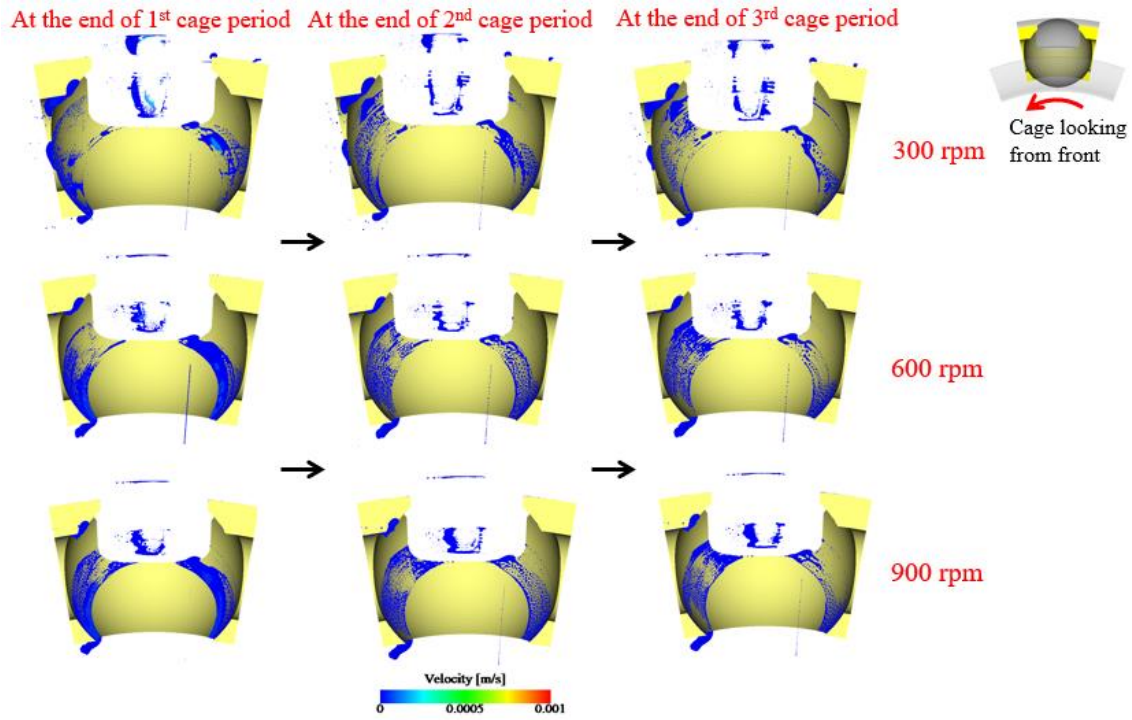

Figure 11. Grease flow in the cage pocket at different speeds (clipped plot).

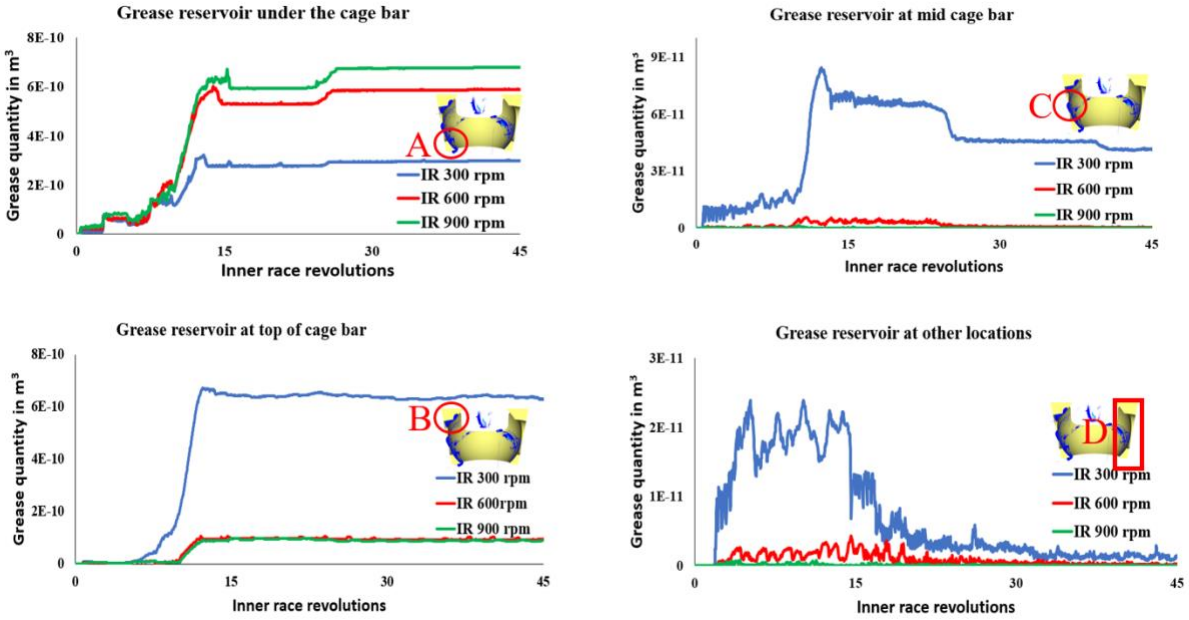

Figure 12. Grease quantity vs Inner race revolutions.

7 Conclusions

A CFD methodology is developed using software Particleworks to predict the formation of grease reservoirs as function of different parameters (e.g. lubricant injection location, rate and speed; bearing operating conditions…). The grease reservoirs are predicted at realistic positions. The bearing rolling elements play a significant role transporting the grease towards the reservoirs. The bearing speed affects the shear rate of the lubricant, which determines its viscosity and ultimately the formation of reservoirs. As an example, the higher the bearing speed, the higher is the amount of grease sticking on the ball, forming a bigger reservoir at the bottom of the cage bar. The presented results focus on a specific injection location, but this methodology can be used with other model settings as well. With this

methodology, the effects of modifications in the bearing component design and lubricant properties on the bearing lubrication conditions can be studied. So, this methodology can support the improvement and the optimisation of the lubrication for rolling bearings.

8 References

[1] P. M. Lugt, “A Review on Grease Lubrication in Rolling Bearings,” Tribology Transactions, vol. 52, no. 4, pp. 470–480, Jun. 2009, doi: https://doi.org/10.1080/10402000802687940.

[2] T. Noda, K. Shibasaki, S. Miyata, and M. Taniguchi, “X-Ray CT Imaging of Grease Behavior in Ball Bearing and Numerical Validation of Multi-Phase Flows Simulation,” Tribology Online, vol. 15, no. 1, pp. 36–44, Feb. 2020, doi: https://doi.org/10.2474/trol.15.36

[3] T. Komoriya et al., “Service Life of Lubricating Grease in Ball Bearings (Part 1) Behavior of Grease and Its Base Oil in a Ball Bearing,” Tribology Online, vol. 16, no. 4, pp. 236–245, Oct. 2021, doi: https://doi.org/10.2474/trol.16.236.

[4] S. Chatra K R and P. M. Lugt, “The process of churning in a grease lubricated rolling bearing: Channeling and clearing,” Tribology International, vol. 153, p. 106661, Jan. 2021, doi: https://doi.org/10.1016/j.triboint.2020.106661.

[5] Particleworks theory manual, release 7.2.0, Prometech software, Inc.

[6] Koshizuka, S. et al. (2018) Moving particle semi-implicit method: A meshfree particle method for fluid dynamics. London, United Kingdom: Academic Press, an imprint of Elsevier.